chemengineering

MDPI

Article

Hydrogen Utilization in Green Fuel Synthesis via CO_2 Conversion to Methanol over New Cu-Based Catalysts

Lorenzo Spadaro [1,2,*], Mariarita Santoro [2], Alessandra Palella [1] and Francesco Arena [1,2]

[1] Institute CNR-TAE "Nicola Giordano", Via Salita S. Lucia 5, I-98126 Messina, Italy; alessandra.palella@itae.cnr.it (A.P.); francesco.arena@unime.it (F.A.)

[2] Dipartimento di Ingegneria, Università di Messina, Viale F. Stagno D'Alcontres 31, I-98166 Messina, Italy; santoro.mariarita@virgilio.it

* Correspondence: lorenzo.spadaro@itae.cnr.it; Tel.: +39-090-624417

Received: 10 November 2017; Accepted: 14 December 2017; Published: 19 December 2017

Abstract: The use of hydrogen as an energy vector and raw material for "very clean liquid fuels" manufacturing has been assessed by the catalytic conversion of CO_2 to methanol over copper based catalysts. A systematic evaluation of copper based catalysts, prepared varying the chemical composition, has been carried out at 0.1–5.0 MPa of total pressure and in the range of 453–513 K by using a semi-automated LAB-microplant, under CO_2/H_2 reactant mixture (1/3), fed at GHSV of 8.8 $NL \cdot kg_{cat}^{-1} \cdot h^{-1}$. Material's properties have been investigated by the means of chemical-physical studies. The findings disclose that the addition of structure promoters (i.e., ZrO_2/CeO_2) strongly improves the textural properties of catalysts, in term of total surface area and exposure of metal surface area (MSA), also reducing the sintering phenomena. The results of the catalytic study clearly prove a structure-activity relationship at low reaction pressure (0.1 MPa), while at higher pressure (3.0–5.0 MPa) the reaction path is insensitive to structure and chemical composition.

Keywords: hydrogen technology; H_2 conversion to liquid fuels; methanol synthesis; CO_2 valorization

1. Introduction

The combined use of CO_2 and renewable H_2, provided by electrolysis or water splitting, in the chemicals and fuels manufacturing, nowadays looks very attractive. In particular, CO_2 conversion into fuel products is the most promising way for a larger H_2 utilization, as an energy vector, providing for instance methanol and other light oxygenated hydrocarbons for fuel cell (FC) applications (i.e., direct methanol/alcohols FC). Indeed, the catalytic hydrogenation of CO_2 is still more effective than direct photo-conversion [1–9].

On the other side, the production of methanol via the hydrogenation of CO_2, using electro-catalytically generated H_2, is of particular interest also for renewable energy concepts, since it can serve as a way to convert and store the excess electrical energy into chemical energy, contributing to smooth the natural fluctuation in the supply of renewable energy [10,11]. Moreover, the CO_2 hydrogenation can contribute to curb CO_2 emissions, which are a cause of the increase in global temperatures and climate change due to the "greenhouse effect" [12].

Prompted by seeking better performing formulations, many authors have explored new catalytic compositions, active in the CO_2 hydrogenation, alternative to the copper-based, such as combinations of Pd [13,14], Au [10,15], or Mo_2C [16,17]. Nevertheless, copper-based catalysts still remain the most suitable catalysts for commercial applications [18]. Cu-based catalysts suffer from detrimental effects of the water produced during catalyst activation and reaction, which inhibits catalytically active sites through the irreversible oxidation of Cu^+ species to Cu^{2+}, leading to a loss of interfacial area and

accelerating the catalyst sintering and the synthesis rate decay [18]. On this address, in the past decades, significant effort has been devoted to improve the properties of Cu-based catalysts by the use of promoters and carriers/supports [19–23]. Several metal oxides are reported in literature for improving the catalytic performance of copper-based catalysts, in term of activity, selectivity, and stability [24–29], also enhancing CO_2 adsorption with respect to un-promoted systems. In particular, in our previous works [30–34], we disclose the positive effects of ZrO_2 on the catalytic performance of Cu-ZnO catalyst with respect to that of Al_2O_3-supported, as a result of the lower hydrophilic nature of ZrO_2 than Al_2O_3, which facilitates water desorption, and its property of stabilizing Cu^+–O species, which favor CO_2 adsorption/activation and methanol selectivity. Then, in more recent studies, we have clearly assessed that ZrO_2 affects structure/morphology and texture of Cu-ZnO based catalysts, while cerium oxides can divalently act as an electronic promoter and improver of surface functionality of Cu phase [33,34].

Therefore, the present work aims to study the combined effects of ZrO_2 and CeO_2 addition on the chemical-physical properties of copper based catalyst, in efforts to shed light on the CO_2 hydrogenation reaction pathways.

2. Materials and Methods

2.1. Synthesis of the Catalysts

Cu–ZnO based catalysts, with a Cu/Zn atomic ratio of circa 3, were prepared by reverse coprecipitation under ultrasound irradiation route, varying $Zr_xCe_{(1-x)}O_2$ carrier composition between $0.2 < x < 0.95$, according to procedure elsewhere described [30]. Table 1 shows the list of catalysts, also reporting the chemical-physical properties.

Table 1. List of catalytic system based on Cu-Zn oxides composites.

Sample		Chemical Composition (wt%)				Physical Properties				
		CuO	ZnO	ZrO_2	CeO_2	SA ($m^2 \cdot g^{-1}$)	PV ($cm^3 \cdot g^{-1}$)	APD [a] (nm)	MSA [c] ($m^2 \cdot g^{-1}$)	MSA/SA_R
CuZn_CZ_100		44.2	13.4	42.1	0.0	154	0.34	9.0	-	-
	R [b]	-	-	-	-	132	0.28	8.0	73	0.55
CuZn_CZ_95		42.8	13.2	38.9	4.2	125	0.40	11.2	-	-
	R [b]	-	-	-	-	62	0.20	12.9	28	0.45
CuZn_CZ_90		42.6	12.8	34.0	8.3	114	0.60	18.7	-	-
	R [b]	-	-	-	-	56	0.21	10.8	25	0.44
CuZn_CZ_50		39.0	12.3	15.6	31.8	80	0.89	48.6	-	-
	R [b]	-	-	-	-	40	0.20	15.7	16	0.40
CuZn_CZ_20		40.1	13.0	5.8	40.3	68	0.32	20.8	-	-
	R [b]	-	-	-	-	36	0.20	21.0	14	0.38
CuZn_CZ_0		38.7	12.2	0.0	48.8	47	0.24	20.0	-	-
	R [b]	-	-	-	-	34	0.17	20.0	10	0.29

(a) Average Pore Diameter (APD, 4PV/SA); (b) sample after reduction treatment at 573 K (1 h) in flowing H_2/Ar and passivation; (c) obtained by "single-pulse" N_2O titration measurements.

2.2. Characterization of the Catalysts

Surface area (SA), pore volume (PV), and average pore diameter (APD) were obtained from nitrogen adsorption/desorption isotherms at 77 K, using ASAP 2020, Micromeritics Instrument. Isotherms were elaborated by the standard BET and BJH methods for SA and PV evaluation, respectively.

X-ray diffraction (XRD) analysis of samples in the 2θ range 10–80° was performed using a Philips X-Pert diffractometer operating with Ni β-filtered Cu Kα radiation at 40 kV and 30 mA.

Metal Surface Area (MSA) values were obtained by measurements of N_2O "single-pulse" titrations, assuming a Cu:N_2O = 2 titration stoichiometry [35,36]. Before measurements, catalysts were reduced

in situ at 573 K in H_2 flow (100 STP mL/min) for 1 h. After reduction, the samples were "washed" in He carrier flow at 583 K for 15 min, and then cooled to 363 K.

2.3. Catalytic Measurements

Catalytic tests were performed at 0.1–5.0 MPa and 453–513 K in a semiautomatic Laboratory microplant, equipped with a AISI 316 stain steel Plug Flow Reactor (i.d., 10 mm; e.d., 12 mm; l., 250 mm), loaded with 1.0 g of catalyst diluted (1/1, wt/wt) with quartz granules (2 mm). Before catalytic tests, catalysts were in-situ activated at 573 K in reducing atmosphere, flowing (5.5 $NL \cdot g^{-1} \cdot h^{-1}$) 5% H_2/Ar gas mixture for 1 h at a heating rate of 10 $K \cdot min^{-1}$. After catalysts activation the reactor was fed with a $CO_2/H_2/N_2$ (3/9/1) mixture flowing at 80 $STPcm^3 \cdot min^{-1}$ (GHSV, 8.800 $NL \cdot kg_{cat}^{-1} \cdot h^{-1}$) using nitrogen as internal standard for GC analysis. The composition of inlet and outlet streams was analyzed in real time by an inline gas chromatograph HP 6890 equipped with a TCD detector and two packed columns (Porapack Q and 5A molecular sieve, Sigma-Aldrich (Milano, Italy)) connected in series for the analysis of permanent gasses, and a FID detector coupled with a capillary column (PoraPLOT Q, i.d., 0.53 mm; l, 30 m, Agilent (Cernusco sul Naviglio (MI), Italy)) for the hydrocarbon species quantification. Methanol and CO were almost the only products formed, while methane and DME are detected only at trace levels (<0.01 mol/mol %).

3. Results

3.1. Chemical-Physical Characterization

As shown in Table 1 and Figure 1, the progressive replacement of $Ce^{3+/4+}$ ions with Zr^{4+} (i.e., $Zr_xCe_{(1-x)}O_2$; 0.2 < x < 0.95) strongly affects both structural and morphological properties of catalysts. Indeed, a remarkable rise of both total and metallic surface area was reported with a consequent increase of the copper–zinc oxide interfacial area, accompanied by an also improved resistance to sintering due to the activation procedure (reduction).

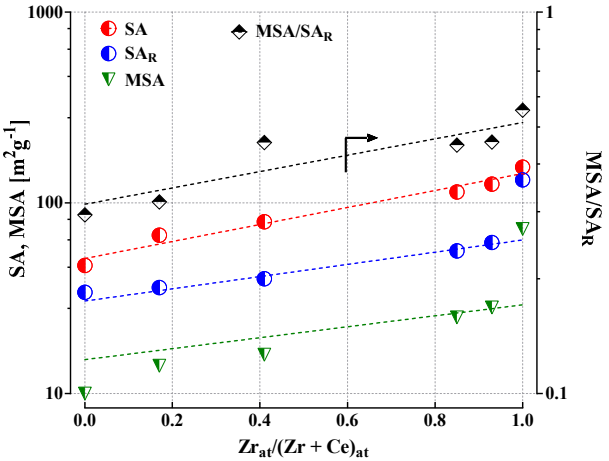

Figure 1. Influence of carrier composition on the textural properties of Cu-Zn based catalysts.

As reported in our previous work [30–32], catalyst activation consists in a controlled reduction to obtain active metallic copper. The action of temperature and H_2 for oxygen removal ($MeO_x + xH_2 \rightarrow xH_2O$; Me = Cu and Ce) leads to the reconstruction of catalyst which can also drive to a higher crystallization with a consequent loss of total surface area (sintering). On this address, the effects of the activation procedure were fully investigated in our previous works [30–32].

In particular, the catalyst without ZrO_2 (CuZn_CZ_0) displays the lowest value of surface area (47 $m^2 \cdot g^{-1}$), which further decreases by 28% after reduction (34 $m^2 \cdot g^{-1}$). By contrast, the system with no CeO_2 (CuZn_CZ_100) shows the highest exposure of total surface (~154 $m^2 \cdot g^{-1}$) and the lowest

decay for the reduction treatment (ΔSA = 14%), confirming the strong effect of zirconia as structural promoter (Figure 1). Indeed, along the replacement of Ce ions in the lattice, the total surface area grows from 67 $m^2 \cdot g^{-1}$ to 125 $m^2 \cdot g^{-1}$, also enhancing MSA value (14–28 $m^2 \cdot g^{-1}$), which mirrors an improved dispersion of active phase, confirmed by an increase of the MSA/SA_R ratio. Then, Figure 2 displays the diffraction patterns of catalysts as prepared (a) and after reduction treatment (b). Irrespective of chemical formulation, XRD analysis signals the lack of "long-range" crystalline order in all samples, due to the ultrasonic preparation method, Figure 2a. In particular, the XRD profile is characterized for all catalysts by the presence of two broad peaks, placed at ca. 31 and 56 2θ degrees, with an increasing intensity at the raise of Zr content. Therefore, catalyst reduction leads to a bulk reconstruction, as shown in Figure 2b. Namely, the catalysts at higher Zr content exhibit the signals of copper in the metallic state, whose most intense reflections appear at 43.3° (<111>) and 50.4° (<200>), respectively. In addition, the occurrence into CuZn_CZ_90 catalyst of sharp peaks, at 35.68° and 38.88°, diagnostics the presence of isolate Tenorite phase (CuO) [JCPDS 5–661], while in the XRD pattern of the reduced CuZn_CZ_95 sample are also evident the diffraction signals of cubic Zirconia [JCPDS 27-0997]. On the other hand, the reflection peaks of metallic Cu are less marked in the reduced samples at lower Zr content (i.e., CuZn_CZ_50 and CuZn_CZ_20), probing a stronger re-oxidation, due to the greater oxygen storage capacity of CeO_2. Furthermore, small intense lines of Zincite phase (ZnO) are detected in the XRD profile of reduced CuZn_CZ_50 catalyst. Therefore, the good chemical stability of catalysts was further proved by results of catalytic test and by XRD analysis on samples after catalytic tests (data not reported here for the sake of brevity).

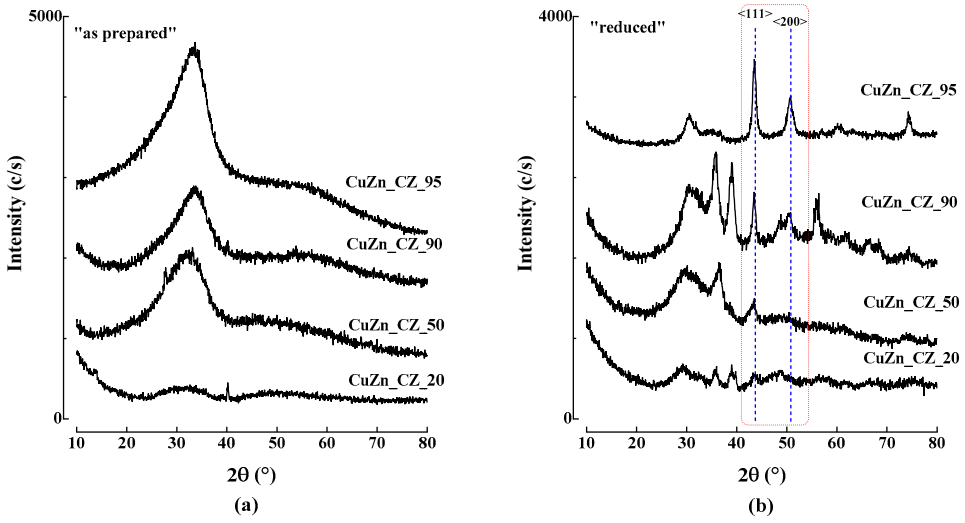

Figure 2. X-ray diffraction (XRD) patterns of Cu-ZnO based catalysts: (**a**) as prepared and (**b**) reduced.

3.2. Catalytic Activity

The results of catalytic tests in the CO_2 hydrogenation in the range of 453–513 K and at 0.1, 3.0 and 5.0 MPa are summarized in Table 2 in terms of H_2 conversion (X_{H_2}%), selectivity to methanol (S_{CH_3OH}%) and reaction rate ($mmolH_2 \cdot h^{-1} \cdot g_{cat}{}^{-1}$).

As extensively reported in literature, CO_2 hydrogenation drives to methanol and CO over Cu-based catalyst through the reactions of methanol synthesis (Equations (1) and (2)) and Reverse Water Gas Shift (Equation (3)), while the methane formation (Equation (4)) is strongly un-favored under such reaction conditions [27,37]:

$$CO_2 + 3H_2 \leftrightarrows CH_3OH + H_2O \quad (1)$$

$$CO + 2H_2 \leftrightarrows CH_3OH \quad (2)$$

$$CO_2 + H_2 \leftrightarrows CO + H_2O \quad (3)$$

$$CO_2 + 4H_2 \leftrightarrows CH_4 + 2H_2O \quad (4)$$

In respect of this, a progressive increase of H_2 conversion, associated with a significant decrease in methanol selectivity, has been observed with the increase in temperature, independent of chemical composition and pressure. According to the greater partial pressure of reactants on the catalyst surface, the H_2 conversion increases further over all samples by upping the pressure from 0.1 MPa to 5.0 MPa. As a rule, ZrO_2 content growth leads to a higher hydrogenation of CO_2, although, the selectivity to methanol is notably reduced.

Table 2. Results of the catalytic test in the CO_2 hydrogenation at different temperature and pressure.

0.1 MPa	X_{H_2} (%)				S_{CH_3OH} (%)				**Reaction Rate (mmolH_2·h^{-1}·$g_{cat}{}^{-1}$)**			
	453 K	**473 K**	**493 K**	**513 K**	**453 K**	**473 K**	**493 K**	**513 K**	**453 K**	**473 K**	**493 K**	**513 K**
CUZN_CZ_100	0.5	1.4	4.9	8.9	34	26	13	3	0.46	1.37	4.85	8.69
CUZN_CZ_95	0.4	2.6	3.6	6.2	56	45	23	7	0.37	2.56	3.57	6.04
CUZN_CZ_90	0.5	2.0	4.1	6.3	71	52	30	11	0.46	1.92	4.02	6.22
CUZN_CZ_20	0.4	1.2	2.8	3.2	77	62	39	19	0.37	1.19	2.74	3.11
CUZN_CZ_0	0.7	1.0	1.9	2.3	96	92	80	61	0.73	1.01	1.83	2.29
3.0 MPa	X_{H_2} (%)				S_{CH_3OH} (%)				**Reaction Rate (mmolH_2·h^{-1}·$g_{cat}{}^{-1}$)**			
	453 K	**473 K**	**493 K**	**513 K**	**453 K**	**473 K**	**493 K**	**513 K**	**453 K**	**473 K**	**493 K**	**513 K**
CUZN_CZ_100	4.1	7.8	13.1	17.7	87	74	57	50	4.02	7.68	12.81	17.38
CUZN_CZ_95	3.5	5.5	7.7	13.1	93	86	65	57	3.38	5.40	7.59	12.81
CUZN_CZ_90	3.5	5.5	9.1	14.9	93	87	71	50	3.38	5.40	8.87	14.63
CUZN_CZ_20	2.9	4.2	6.0	7.9	94	90	82	69	2.84	4.12	5.85	7.77
CUZN_CZ_0	1.9	3.2	4.8	6.7	97	95	90	80	1.83	3.11	4.66	6.59
5.0 MPa	X_{H_2} (%)				S_{CH_3OH} (%)				**Reaction Rate (mmolH_2·h^{-1}·$g_{cat}{}^{-1}$)**			
	453 K	**473 K**	**493 K**	**513 K**	**453 K**	**473 K**	**493 K**	**513 K**	**453 K**	**473 K**	**493 K**	**513 K**
CUZN_CZ_100	5.3	9.3	15.9	20.5	90	78	65	64	5.21	9.15	15.55	20.12
CUZN_CZ_95	4.4	6.3	9.3	14.9	93	89	74	54	4.30	6.22	9.15	14.63
CUZN_CZ_90	4.1	6.7	10.3	15.9	94	87	76	56	4.02	6.59	10.06	15.55
CUZN_CZ_20	3.8	5.2	6.9	9.1	94	91	86	74	3.75	5.12	6.77	8.96
CUZN_CZ_0	2.1	3.7	6.1	7.9	97	95	90	81	2.01	3.66	5.95	7.77

In particular, reaction rate raises from 8.7 mmol·h^{-1}·$g_{cat}{}^{-1}$ to the greater 20.1 mmol·h^{-1}·$g_{cat}{}^{-1}$ at the highest temperature (513 K), moving from 0.1 MPa to 5.0 MPa by using the most active catalyst (CuZn_CZ_100). While the reaction rate increases only in the range of 2.3–7.8 (mmol·h^{-1}·$g_{cat}{}^{-1}$), at the same test condition, employing the less active catalyst (CuZn_CZ_0).

In catalysis, "Activation Energy" counts for the energy that must be supplied to catalyst to observe any chemical reaction. On this account, a further evaluation of the effects of carrier composition on the catalytic functionality of Cu-ZnO systems can be done comparing the values of Apparent Activation Energy (E_{app} (kJ·mol^{-1})), obtained from the Arrhenius's plot of differential conversion data at 0.1 MPa (X_{H_2} < 10%, T = 453–513 K), reported in Figure 3 [30,31,38]. Indeed, the progressive increase of CeO_2 content leads to a decrease in E_{app} value from 97 kJ·mol^{-1} of CuZn_CZ_0 sample to 26 kJ·mol^{-1} of CuZn_CZ_100 system, as proof of the promoter effect of ceria. The catalytic data at higher pressure (i.e., 3.0 and 5.0 MPa) were not considered for the evaluation of E_{app}, because the hydrogen conversion (X_{H_2}) overcame the value of 10%.

As well known, at the kinetic regime, the value of the Apparent Activation Energy (E_{app}) is directly related to the kinetic constant "K" and, consequently, to the reaction rate (rate $\propto$ K) through Arrhenius's Law, also reflecting the energies needed for the chemisorption and desorption processes of the molecule on the surface of active sites [39,40]. Therefore, the decreasing in the value of E_{app} observed with the raise of Ceria contents in the catalyst formulation can also mirror a more favorable chemisorption or desorption steps in the hydrogenation reaction.

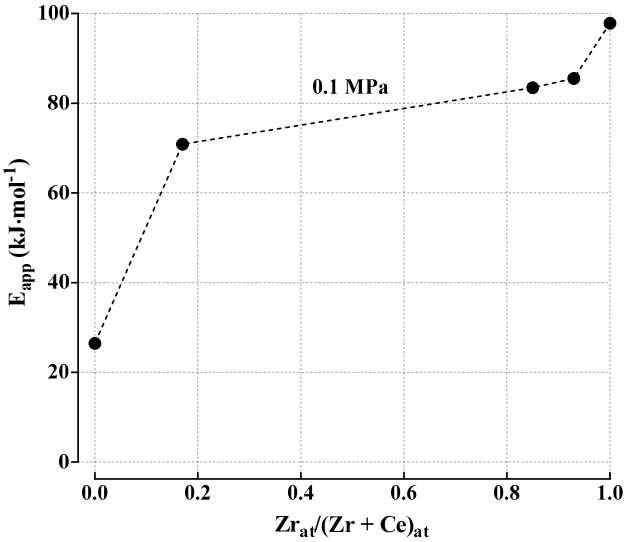

Figure 3. Apparent activation energy (E_{app}) of Cu–ZnO catalysts at 0.1 MPa.

4. Discussion

CO_2 hydrogenation to methanol by using Cu-based catalytic systems promoted by several oxides/carriers has been widely investigated in literature [3,5,16–24,27–32], although very few examples of multicomponent CuO-ZnO-CeO_2 and CuO-ZnO-CeO_2-ZrO_2 systems are still present [25,26,33,34,41,42].

Cerium oxides are well recognized catalytic materials for the oxygen storage capacity of Ceria and for several features such as to be an enhancer of active phase dispersion, for weakening the C–O bond and for improving the chemisorption of H_2 [43–45]. As an electronic promoter, Ceria also plays a crucial role in the behavior of the catalyst, thanks to its peculiar reactivity [43,44]. In this work, the effect of catalyst formulation becomes more clear by plotting the logarithm of H_2 conversion (lgX_{H_2}) against the selectivity to methanol, Figure 4. Namely, at 0.1 MPa the catalytic behavior of all catalysts can be described through three different curves of activity, which respond to different catalyst formulation. Differently, at the higher pressure (3.0 and 5.0 MPa) the samples exhibit similar catalytic paths. These findings suggest that catalyst chemisorption capacity, also with respect to intermediate products, could affect the catalytic behavior at low reactants coverage. In particular, at 0.1 MPa the catalyst with composition "Cu-ZnO-ZrO_2" (CuZn_CZ_100) promotes mainly the reaction of hydrogenation which leads to form CO. By contrast, the catalyst with the chemical formulation "Cu-ZnO-CeO_2" (CuZn_CZ_0) favors mainly the methanol synthesis, perhaps, thanks to the oxygen storage capacity of Ceria. Indeed, according to the reaction mechanism in which methanol synthesis occurs via hydrogenation of a "bridge-formate" intermediate [46,47], CuZn_CZ_0 would promote methanol because of its higher capacity to weaken and bend C–O bonds. In addition, the higher hydrogen coverage on the surface, due to the H_2-spillover phenomena, could further enhance the selectivity to methanol for CuZn_CZ_0 catalyst. Therefore, the catalytic behavior held by the catalysts having both ZrO_2 and CeO_2 promoter/carrier results in a right equilibrium of chemical-physical properties of the two different oxides, being a good compromise between the two extreme catalytic performance.

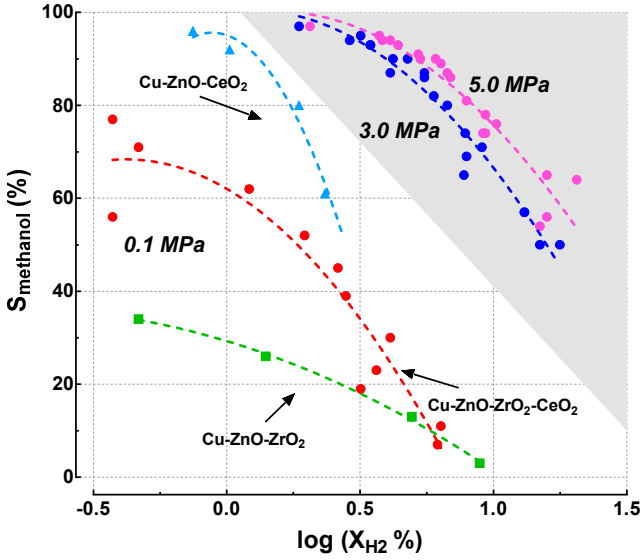

Figure 4. Activity pattern in the CO_2 hydrogenation reaction.

Therefore, the effects of ceria, as structural and electronic promoter, can be both at level of solid-state interactions and reactivity toward reactant gas [30–34,45,48], affecting the redox and electronic properties of the active phase and modelling the adsorption behavior. On the other hand, the enhanced reducibility (data not here reported) and the well stated surface affinity for H_2 can further justify the lower value of Apparent Activation Energy [30–34,45,48].

Then, to shed light on structure-activity relationship, the catalytic results were analyzed according to their textural properties (SA and MSA). On this account, Figure 5a,b reports reaction rate and "normalized methanol yield" at 5.0 MPa and at varying of MSA and MSA/SA_R values, respectively. In particular, the CO_2 hydrogenation rate increases almost proportionally with the increase of metal exposure, Figure 5a, according to the consistent rise and reconstruction of the active phases/sites ($Cu^0 \leftrightarrows Cu^+$). On the other side, Figure 1 and Table 1 shown that the value of MSA increases by the growth of the atomic fraction of Zr, as proof of the greater efficacy of ZrO_2 carrier as structural promoter and improver of metal dispersion. Moreover, methanol synthesis over Cu-based catalyst is characterized by a "dual site mechanism", which invokes a right equilibrium between Cu^+ and Cu^0 active sites, according to the following equation 5:

$$rate_{methanol} = K \cdot [CO_2] \cdot [H_2] \propto K \cdot [Cu^{(I)}] \cdot [Cu^{(0)}] \quad (5)$$

where a greater concentration of Cu^0 sites drive to high hydrogen supply on the catalytic surface, while a major exposition of Cu^+ active sites on SA strongly enhance CO_2 chemisorption. Therefore, the catalyst performance depends on the right "deal" between the two catalytic functionalities [3,38,45,46,49–51].

In other words, all "Cu-ZnO-ZrO_2-CeO_2" catalysts obey the occurrence of a similar "dual-site" reaction path that is a mechanism with two active centers involved in the catalytic process of CO_2 hydrogenation. The first one should be the oxide phase, with basic properties, which attends to adsorb and activate CO_2 molecules for running hydrogenation to methanol, through the formation of a formate as intermediate [46]. In more detail, the CO_2 chemisorption can occur both via Zirconia Lewis basic sites [47,49,50], as well as by action of metal alkaline ZnO phase which enhances the affinity of $Cu^{(+)}$–O to CO_2 [18]. As proof, in our previous works we have attested a larger CO_2 uptake, consequently to a greater concentration of basic sites [33,34]. On the other hand, the other sites should accomplish the adsorption and dissociation of H_2 molecules for the reaction with CO_2 [24,47]. On this account, the occurring of a reaction pathway which involves the existence of two kind of reaction sites

is confirmed for "Cu-ZnO-ZrO_2-CeO_2" catalytic systems by a "volcano-shape" relationship, obtained by plotting normalized methanol yield versus the ratio MSA/SA_R, here used as an indirect index of the dual-sites equilibrium (Figure 5b). Namely, the wide range of values assumed by the normalized yield at the varying of MSA/SA_R discloses the structure-activity relationship of these catalytic materials, and at the same time, reflects the effect of chemical composition. In addition, the existence of a maximum value of methanol yield, which should be achieved at 5.0 MPa at an "ideal" ratio of MSA/SA_R near to 0.3, clearly signs the need of a perfect synergism between the two catalytic functionalities, available through a proper design of the catalyst [51–54].

In particular, despite the lower activity, the use of Ceria in combination with Zirconia leads to a more favorable Activation Energy (ranging from 97 to 27 kJ·mol^{-1}), which also results in higher values of methanol yield than that of the sample with no Ceria. In other words, even the addition of small quantities of CeO_2 as promoter (i.e., 5–10 wt%) confers to catalyst a peculiar reactivity towards the methanol formation, by enhancing the surface functionality of Cu-ZnO-ZrO_2 system.

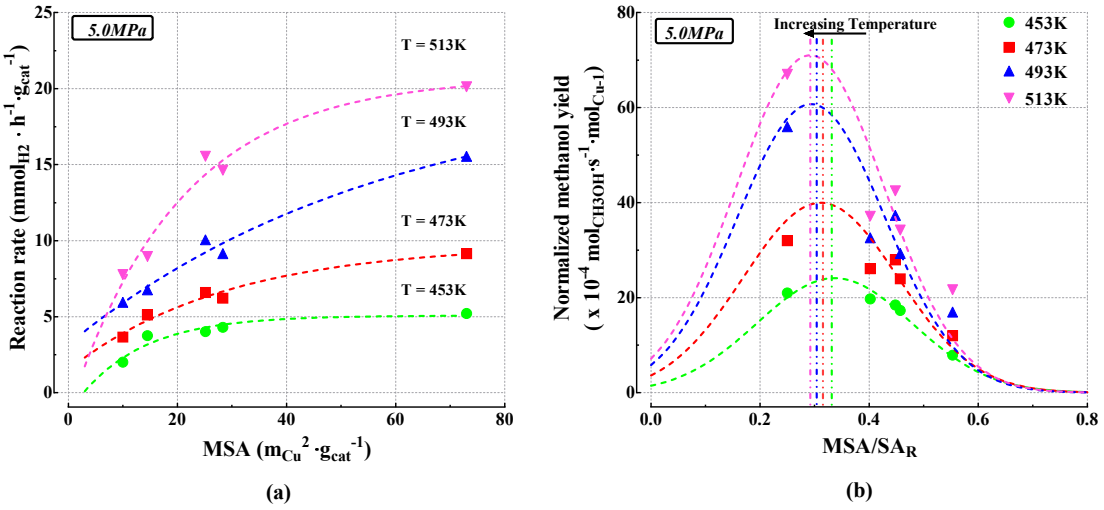

Figure 5. Structure-reactivity relationships for Cu-ZnO catalysts: (**a**) Reaction rate as function of MSA at 5.0 MPa; (**b**) Normalized methanol yield vs. MSA/SA_R at 5.0 MPa.

These findings concur well with our earlier results, especially in term of methanol yield and E_{app} [30–34]. In addition, the catalytic performance of CuO-ZnO-CeO_2-ZrO_2 systems represent an advancement with respect to the results recently reported in literature by Cu-based catalysts [26,41,42].

5. Conclusions

The catalytic performance in CO_2 hydrogenation process for a series of new "Cu-ZnO-ZrO_2-CeO_2" catalysts have been assessed, approaching real industrial process conditions.

The work assessed the effect of chemical composition and preparation method regarding the sintering phenomena due to the activation procedure (reduction) in which the action of temperature and H_2 in the oxygen removing and metallic copper formation ($MeO_x + xH_2 = xH_2O$; Me = Cu and Ce). This leads to catalyst reconstruction which can also drive to higher crystallization with a consequent loss of total surface area. The progressive replacement of $Ce^{3+/4+}$ ions with Zr^{4+} (i.e., $Zr_xCe_{(1-x)}O_2$; $0.2 < x < 0.95$) has been proved affecting both SA and MSA exposure, improving also the resistance to sintering phenomena.

The progressive increase of CeO_2 content has been ascertained to lead to a more favorable Activation Energy values. The results obtained with CuO-ZnO-CeO_2-ZrO_2 systems represent a further advancement in the comprehension of catalytic pathway of Cu-based catalyst, The "dual-site" mechanism, as reaction pathway in methanol synthesis, has been confirmed, through a

"volcano-shape" relationship, obtained between hydrogenation activity and catalytic structure of "Cu-ZnO-ZrO_2-CeO_2" systems.

The addition of even low quantities of CeO_2 (i.e., 5–10%) allows one to obtain materials with enhanced chemical properties, maintaining the striking structural promoter effect of ZrO_2, and, at the same time, introducing the functionality of CeO_2, with a satisfactory compromise between activity and selectivity.

Author Contributions: Lorenzo Spadaro and Francesco Arena conceived and designed the experiments and supervised the research activity. Mariarita Santoro and Alessandra Palella performed the experiments and analyzed the experimental data. All the authors participated to the discussion of the results and to the drafting of the paper.

Conflicts of Interest: The authors declare no conflict of interest.

References

1. Saeidi, S.; Amin, N.A.S.; Rahimpour, M.R. Hydrogenation of CO_2 to value-added products—A review and potential future developments. *J. CO_2 Util.* **2014**, *5*, 66–81. [CrossRef]
2. Larson, E.D.; Tingjin, R. Synthetic fuel production by indirect coal liquefaction. *Energy Sustain. Dev.* **2003**, *7*, 79–102. [CrossRef]
3. Liu, X.-M.; Lu, G.Q.; Yan, Z.-F.; Beltramini, J. Recent Advances in Catalysts for Methanol Synthesis via Hydrogenation of CO and CO_2. *Ind. Eng. Chem. Res.* **2003**, *42*, 6518–6530. [CrossRef]
4. Song, C. Global challenges and strategies for control, conversion and utilization of CO_2 for sustainable development involving energy, catalysis, adsorption and chemical processing. *Catal. Today* **2006**, *115*, 2–32. [CrossRef]
5. Wang, W.; Wang, S.; Ma, X.; Gong, J. Recent advances in catalytic hydrogenation of carbon dioxide. *Chem. Soc. Rev.* **2011**, *40*, 3703. [CrossRef] [PubMed]
6. Fiedler, E.; Grossmann, G.; Kersebohm, D.B.; Weiss, G.; Witte, C. Methanol. In *Ullmann's Encyclopedia of Industrial Chemistry*; Wiley: New York, NY, USA, 2000.
7. Chen, C.-Y.; Yu, J.C.-C.; Nguyen, V.-H.; Wu, J.C.-S.; Wang, W.-H.; Kočí, K. Reactor Design for CO_2 Photo-Hydrogenation toward Solar Fuels under Ambient Temperature and Pressure. *Catalysts* **2017**, *7*, 63. [CrossRef]
8. Olah, G.A.; Goeppert, A.; Prakash, G.K.S. Chemical recycling of carbon dioxide to methanol and dimethyl ether: From greenhouse gas to renewable environmentally carbon neutral fuels and synthetic hydrocarbons. *J. Org. Chem.* **2009**, *74*, 487–498. [CrossRef] [PubMed]
9. Pontzen, F.; Liebner, W.; Gronemann, V.; Rothaemel, M.; Ahlers, B. CO_2-based methanol and DME—Efficient technologies for industrial scale production. *Catal. Today* **2011**, *171*, 242–250. [CrossRef]
10. Hartadi, Y.; Widmann, D.; Behm, R.J. Methanol formation by CO_2 hydrogenation on Au/ZnO catalysts—Effect of total pressure and influence of CO on the reaction characteristics. *J. Catal.* **2016**, *333*, 238–250. [CrossRef]
11. Schlögl, R. Chemistry's Role in Regenerative Energy. *Angew. Chem.-Int. Ed.* **2011**, *50*, 6424–6426. [CrossRef] [PubMed]
12. Larminie, J.; Dicks, A. *Fuel Cell Systems Explained*, 2nd ed.; Wiley: New York, NY, USA, 2003.
13. Jiang, X.; Koizumi, N.; Guo, X.; Song, C. Bimetallic Pd-Cu catalysts for selective CO_2 hydrogenation to methanol. *Appl. Catal. B Environ.* **2015**, *170–171*, 173–185. [CrossRef]
14. Rui, N.; Wang, Z.; Sun, K.; Ye, J.; Ge, Q.; Liu, C.J. CO_2 hydrogenation to methanol over Pd/In_2O_3: Effects of Pd and oxygen vacancy. *Appl. Catal. B Environ.* **2017**, *218*, 488–497. [CrossRef]
15. Vourros, A.; Garagounis, I.; Kyriakou, V.; Carabineiro, S.A.C.; Maldonado-Hódar, F.J.; Marnellos, G.E.; Konsolakis, M. Carbon dioxide hydrogenation over supported Au nanoparticles: Effect of the support. *J. CO_2 Util.* **2017**, *19*, 247–256. [CrossRef]
16. Ma, Y.; Guan, G.; Hao, X.; Cao, J.; Abudula, A. Molybdenum carbide as alternative catalyst for hydrogen production—A review. *Renew. Sustain. Energy Rev.* **2017**, *75*, 1101–1129. [CrossRef]
17. Liu, X.; Song, Y.; Geng, W.; Li, H.; Xiao, L.; Wu, W. Cu-Mo_2C/MCM-41: An Efficient Catalyst for the Selective Synthesis of Methanol from CO_2. *Catalysts* **2016**, *6*, 75. [CrossRef]

18. Arena, F.; Mezzatesta, G.; Spadaro, L.; Trunfio, G. Latest advances in the catalytic hydrogenation of CO_2 to methanol/dimethylether. In *Transformation and Utilization of Carbon Dioxide, Green Chemistry and Sustainable Technology*; Bhanage, B.M., Arai, M., Eds.; Springer: Berlin/Heidelberg, Germany, 2014. [CrossRef]
19. Jadhav, S.G.; Vaidya, P.D.; Bhanage, B.M.; Joshi, J.B. Catalytic carbon dioxide hydrogenation to methanol: A review of recent studies. *Chem. Eng. Res. Des.* **2014**, *92*, 2557–2567. [CrossRef]
20. Deng, K.; Hu, B.; Lu, Q.; Hong, X. Cu/g-C3N4 modified ZnO/Al_2O_3 catalyst: Methanol yield improvement of CO_2 hydrogenation. *Catal. Commun.* **2017**, *100*, 81–84. [CrossRef]
21. Li, S.M.M.-J.; Zeng, Z.; Liao, F.; Hong, H.; Tsang, S.C.E. Enhanced CO_2 hydrogenation to methanol over CuZn nanoalloy in Ga modified Cu/ZnO catalysts. *J. Catal.* **2016**, *343*, 157–163. [CrossRef]
22. Umegaki, T.; Kojima, Y.; Omata, K. Effect of oxide coating on performance of copper-zinc oxide-based catalyst for methanol synthesis via hydrogenation of carbon dioxide. *Materials* **2015**, *8*, 7738–7744. [CrossRef] [PubMed]
23. Da Silva, R.J.; Pimentel, A.F.; Monteiro, R.S.; Mota, C.J.A. Synthesis of methanol and dimethyl ether from the CO_2 hydrogenation over Cu/ZnO supported on Al_2O_3 and Nb_2O_5. *J. CO_2 Util.* **2016**, *15*, 83–88. [CrossRef]
24. Xiao, J.; Mao, D.; Guo, X.; Yu, J. Effect of TiO_2, ZrO_2, and TiO_2-ZrO_2 on the performance of CuO-ZnO catalyst for CO_2 hydrogenation to methanol. *Appl. Surf. Sci.* **2015**, *338*, 146–153. [CrossRef]
25. Chang, K.; Wang, T.; Chen, J.C. Hydrogenation of CO_2 to methanol over $CuCeTiO_x$ catalysts. *Appl. Catal. A Gen.* **2017**, *206*, 704–711. [CrossRef]
26. Ouyang, B.; Tan, W.; Liu, B. Morphology effect of nanostructure ceria on the Cu/CeO_2 catalysts for synthesis of methanol from CO_2 hydrogenation. *Catal. Commun.* **2017**, *95*, 36–39. [CrossRef]
27. Gao, P.; Li, F.; Zhan, H.; Zhao, N.; Xiao, F.; Wei, W.; Zhong, L.; Wang, H.; Sun, Y. Influence of Zr on the performance of Cu/Zn/Al/Zr catalysts via hydrotalcite-like precursors for CO_2 hydrogenation to methanol. *J. Catal.* **2013**, *298*, 51–60. [CrossRef]
28. Gao, P.; Li, F.; Zhan, H.; Zhao, N.; Xiao, F.; Wei, W.; Zhong, L.; Sun, Y. Fluorine-modified Cu/Zn/Al/Zr catalysts via hydrotalcite-like precursors for CO_2 hydrogenation to methanol. *Catal. Commun.* **2014**, *50*, 78–82. [CrossRef]
29. Huang, C.; Chen, S.; Fei, X.; Liu, D.; Zhang, Y. Catalytic Hydrogenation of CO_2 to Methanol: Study of Synergistic Effect on Adsorption Properties of CO_2 and H_2 in CuO/ZnO/ZrO_2 System. *Catalysts* **2015**, *5*, 1846–1861. [CrossRef]
30. Arena, F.; Barbera, K.; Italiano, G.; Bonura, G.; Spadaro, L.; Frusteri, F. Synthesis, characterization and activity pattern of Cu-ZnO/ZrO_2 catalysts in the hydrogenation of carbon dioxide to methanol. *J. Catal.* **2007**, *249*, 185–194. [CrossRef]
31. Arena, F.; Italiano, G.; Barbera, K.; Bordiga, S.; Bonura, G.; Spadaro, L.; Frusteri, F. Solid-state interactions, adsorption sites and functionality of Cu-ZnO/ZrO_2 catalysts in the CO_2 hydrogenation to CH_3OH. *Appl. Catal. A Gen.* **2008**, *350*, 16–23. [CrossRef]
32. Arena, F.; Italiano, G.; Barbera, K.; Bonura, G.; Spadaro, L.; Frusteri, F. Basic evidences for methanol-synthesis catalyst design. *Catal. Today* **2009**, *143*, 80–85. [CrossRef]
33. Arena, F.; Mezzatesta, G.; Zafarana, G.; Trunfio, G.; Frusteri, F.; Spadaro, L. How oxide carriers control the catalytic functionality of the Cu-ZnO system in the hydrogenation of CO_2 to methanol. *Catal. Today* **2013**, *210*, 39–46. [CrossRef]
34. Arena, F.; Mezzatesta, G.; Zafarana, G.; Trunfio, G.; Frusteri, F.; Spadaro, L. Effects of oxide carriers on surface functionality and process performance of the Cu-ZnO system in the synthesis of methanol via CO_2 hydrogenation. *J. Catal.* **2013**, *300*, 141–151. [CrossRef]
35. Agrell, J.; Birgersson, H.; Boutonnet, M.; Melián-Cabrera, I.; Navarro, R.M.; Fierro, J.L.G. Production of hydrogen from methanol over Cu/ZnO catalysts promoted by ZrO_2 and Al_2O_3. *J. Catal.* **2003**, *219*, 389–403. [CrossRef]
36. Evans, J.W.; Wainwright, M.S.; Bridgewater, A.J.; Young, D.J. On the determination of copper surface area by reaction with nitrous oxide. *Appl. Catal.* **1983**, *7*, 75–83. [CrossRef]
37. Zhang, L.; Zhang, Y.; Chen, S. Effect of promoter SiO_2, TiO_2 or SiO_2-TiO_2 on the performance of CuO-ZnO-Al_2O_3 catalyst for methanol synthesis from CO_2 hydrogenation. *Appl. Catal. A Gen.* **2012**, *415–416*, 118–123. [CrossRef]

38. Arena, F.; Di Chio, R.; Fazio, B.; Espro, C.; Spiccia, L.; Palella, A.; Spadaro, L. Probing the functionality of nanostructured MnCeOx catalysts in the carbon monoxide oxidation. Part I. Influence of cerium addition on structure and CO oxidation activity. *Appl. Catal. B Environ.* **2017**, *210*, 14–22. [CrossRef]
39. Chorkendorff, I.; Niemantsverdiet, J.W. *Concepts of Modern Catalysis and Kinetics*; Wiley-VCH Verlag GmgH & Co. KGaA: Weinheim, Germany, 2007.
40. Bartholomew, C.H.; Ferrauto, R.J. *Foundamentals of Industrial Catalytic Processes*; Wiley-Interscience: Hoboken, NJ, USA, 2006.
41. Li, L.; Mao, D.; Yu, J.; Guo, X. Highly selective hydrogenation of CO_2 to methanol over CuO-ZnO-ZrO_2 catalysts prepared by a surfactant-assisted co-precipitation method. *J. Power Sources* **2015**, *279*, 394–404. [CrossRef]
42. Angelo, L.; Kobl, K.; Tejada, L.M.M.; Zimmermann, Y.; Parkhomenko, K.; Roger, A.-C. Study of $CuZnMO_x$ oxides (M = Al, Zr, Ce, CeZr) for the catalytic hydrogenation of CO_2 into methanol. *C. R. Chim.* **2015**, *18*, 250–260. [CrossRef]
43. Arena, F.; Famulari, P.; Trunfio, G.; Bonura, G.; Frusteri, F.; Spadaro, L. Probing the factors affecting structure and activity of the Au/CeO_2 system in total and preferential oxidation of CO. *Appl. Catal. B Environ.* **2006**, *66*, 81–91. [CrossRef]
44. Arena, F.; Famulari, P.; Interdonato, N.; Bonura, G.; Frusteri, F.; Spadaro, L. Physico-chemical properties and reactivity of Au/CeO_2 catalysts in total and selective oxidation of CO. *Catal. Today* **2006**, *116*, 384–390. [CrossRef]
45. Trovarelli, A. *Catalysis by Ceria and Related Materials*; Imperial College Press: London, UK, 2002.
46. Kunkes, E.L.; Studt, F.; Abild-Pedersen, F.; Schlögl, R.; Behrens, M. Hydrogenation of CO_2 to methanol and CO on Cu/ZnO/Al_2O_3: Is there a common intermediate or not? *J. Catal.* **2015**, *328*, 43–48. [CrossRef]
47. Fisher, I.A.; Bell, A.T. *In-Situ* Infrared Study of Methanol Synthesis from H_2/CO_2 over Cu/SiO_2 and Cu/ZrO_2/SiO_2. *J. Catal.* **1997**, *172*, 222–237. [CrossRef]
48. Spadaro, L.; Arena, F.; Granados, M.L.; Ojeda, M.; Fierro, J.L.G.; Frusteri, F. Metal-support interactions and reactivity of Co/CeO_2 catalysts in the Fischer-Tropsch synthesis reaction. *J. Catal.* **2005**, *234*, 451–462. [CrossRef]
49. Fisher, I.A.; Bell, A.T. *In-Situ* Infrared Study of Methanol Synthesis from H_2/CO over Cu/SiO_2 and Cu/ZrO_2/SiO_2. *J. Catal.* **1998**, *178*, 153–173. [CrossRef]
50. Pokrovski, K.; Jung, K.T.; Bell, A.T. Investigation of CO and CO_2 Adsorption on Tetragonal and Monoclinic Zirconia. *Langmuir* **2001**, *17*, 4297–4303. [CrossRef]
51. Tada, S.; Watanabe, F.; Kiyota, K.; Shimoda, N.; Hayashi, R.; Takahashi, M.; Nariyuki, A.; Igarashi, A.; Satokawa, S. Ag addition to CuO-ZrO_2 catalysts promotes methanol synthesis via CO_2 hydrogenation. *J. Catal.* **2017**, *351*, 107–118. [CrossRef]
52. Bahruji, H.; Bowker, M.; Hutchings, G.; Dimitratos, N.; Wells, P.; Gibson, E.; Jones, W.; Brookes, C.; Morgan, D.; Lalev, G. Pd/ZnO catalysts for direct CO_2 hydrogenation to methanol. *J. Catal.* **2016**, *343*, 133–146. [CrossRef]
53. Yang, C.; Ma, Z.; Zhao, N.; Wei, W.; Hu, T.; Sun, Y. Methanol synthesis from CO_2-rich syngas over a ZrO_2 doped CuZnO catalyst. *Catal. Today* **2006**, *115*, 222–227. [CrossRef]
54. Ma, Y.; Sun, Q.; Wu, D.; Fan, W.-H.; Zhang, Y.-L.; Deng, J.-F. A practical approach for the preparation of high activity Cu/ZnO/ZrO_2 catalyst for methanol synthesis from CO_2 hydrogenation. *Appl. Catal. A Gen.* **1998**, *171*, 45–55. [CrossRef]